The Plant Cell, Vol. 26: 280–295, January 2014, www.plantcell.org

AUXIN BINDING PROTEIN1 Links Cell Wall Remodeling, Auxin Signaling, and Cell Expansion in *Arabidopsis*[W]

Sébastien Paque,[a] Grégory Mouille,[b] Laurie Grandont,[a] David Alabadí,[c] Cyril Gaertner,[b] Arnaud Goyallon,[b] Philippe Muller,[a] Catherine Primard-Brisset,[a] Rodnay Sormani,[b] Miguel A. Blázquez,[c] and Catherine Perrot-Rechenmann[a,1]

[a] Institut des Sciences du Végétal, UPR2355, CNRS, Saclay Plant Sciences, 91198 Gif sur Yvette Cedex, France
[b] Institut Jean-Pierre Bourgin, Saclay Plant Sciences, INRA Centre de Versailles-Grignon, 78026 Versailles Cedex, France
[c] Instituto de Biología Molecular y Celular de Planta, Consejo Superior de Investigaciones Científicas, Universitat Politécnica de Valencia, 46022 Valencia, Spain

Cell expansion is an increase in cell size and thus plays an essential role in plant growth and development. Phytohormones and the primary plant cell wall play major roles in the complex process of cell expansion. In shoot tissues, cell expansion requires the auxin receptor AUXIN BINDING PROTEIN1 (ABP1), but the mechanism by which ABP1 affects expansion remains unknown. We analyzed the effect of functional inactivation of ABP1 on transcriptomic changes in dark-grown hypocotyls and investigated the consequences of gene expression on cell wall composition and cell expansion. Molecular and genetic evidence indicates that ABP1 affects the expression of a broad range of cell wall–related genes, especially cell wall remodeling genes, mainly via an $SCF^{TIR/AFB}$-dependent pathway. ABP1 also functions in the modulation of hemicellulose xyloglucan structure. Furthermore, fucosidase-mediated defucosylation of xyloglucan, but not biosynthesis of nonfucosylated xyloglucan, rescued dark-grown hypocotyl lengthening of ABP1 knockdown seedlings. In muro remodeling of xyloglucan side chains via an ABP1-dependent pathway appears to be of critical importance for temporal and spatial control of cell expansion.

INTRODUCTION

The essential protein AUXIN BINDING PROTEIN1 (ABP1) functions in the control of growth and development throughout plant life. Initially identified by its capacity to bind the phytohormone auxin, ABP1 was first shown to affect plasma membrane hyperpolarization via the modulation of ion fluxes across the membrane (Thiel et al., 1993; Barbier-Brygoo et al., 1996; Leblanc et al., 1999a, 1999b). These rapid ionic changes indicate a possible involvement of ABP1 in the control of cell expansion, at least in shoot tissues, thus providing preliminary molecular evidence supporting the acid growth theory. This theory states that auxin promotes the excretion of protons at the apoplast resulting in cell wall loosening and increased growth rate (Rayle and Cleland, 1992). Binding of auxin to ABP1 and increased amount of ABP1 at the plasma membrane promote protoplast swelling and enhance expansion of leaf cells (Jones et al., 1998; Steffens et al., 2001; Christian et al., 2006). Conversely, the functional inactivation of ABP1 severely impairs cell expansion in shoot tissues irrespective of their DNA content (Braun et al., 2008; Xu et al., 2010) but does not affect root cell elongation (Tromas et al., 2009). The effect of ABP1 on cell expansion varies in a cell- or tissue-dependent manner. Recent data indicate that ABP1 acts both constitutively and in response to auxin (Robert et al., 2010; Tromas et al., 2013). The mechanism by which ABP1 controls cell expansion remains poorly understood. In shoot tissues, it remains unclear whether the contribution of ABP1 to cell expansion relies solely on nongenomic responses or acts also via the regulation of gene expression. ABP1 was reported to affect expression of various genes in response to auxin, but little is known on the broader effects of ABP1 on gene expression (Braun et al., 2008; Tromas et al., 2009; Effendi et al., 2011).

Recent work showed that ABP1 constitutively controls the stability of AUXIN/INDOLE-3-ACETIC ACID (AUX/IAA) transcriptional repressors and negatively regulates the $SCF^{TIR1/AFB}$ pathway (Tromas et al., 2013). The $SCF^{TIR1/AFB}$ pathway includes various combinations of TRANSPORT INHIBITOR1/AUXIN SIGNALING F-BOX (TIR1/AFB) and AUX/IAA nuclear-localized coreceptors, which have distinct relative affinities for auxin binding or distinct specificities (Calderón Villalobos et al., 2012). TIR1/AFB F-box proteins promote polyubiquitination of AUX/IAA substrates and their degradation via the 26S proteasome (Chapman and Estelle, 2009). After degradation of AUX/IAA repressors, AUXIN RESPONSE FACTORs regulate the transcription of auxin responsive genes. ABP1 and $SCF^{TIR1/AFB}$ signaling pathways ensure highly controlled and balanced responses to changes in auxin concentration during plant growth and development.

Cell expansion is an increase in cell size and thus plays an essential role in plant growth and adaptive processes. Expansion results from complex mechanisms, and the ability of cell walls to extend is both important and potentially restrictive (Wolf et al., 2012). Expansion requires cell wall loosening, which involves modification and remodeling of cell wall components and biosynthesis

[1] Address correspondence to catherine.rechenmann@isv.cnrs-gif.fr.
The author responsible for distribution of materials integral to the findings presented in this article in accordance with the policy described in the Instructions for Authors (www.plantcell.org) is: Catherine Perrot-Rechenmann (catherine.rechenmann@isv.cnrs-gif.fr).
[W] Online version contains Web-only data.
www.plantcell.org/cgi/doi/10.1105/tpc.113.120048

of new cell wall materials. In growing cells, crystalline cellulose microfibrils and hemicelluloses of the primary cell wall interact to form a complex network comparable to an external skeleton surrounding the plant cells. In dicots, this network is embedded in a gel of pectin that contains proteins involved either in cell wall loosening or in the integration of novel cell wall components within the network. Composition and physical properties of the primary cell wall are highly regulated to control growth according to the organ and in response to developmental or environmental stimuli.

In most vascular dicotyledonous plants, xyloglucan polysaccharides (XyGs) constitute the major hemicellulose (Harholt et al., 2006). XyGs have a backbone of β-1,4-D-glucopyranosyl and a combination of side chains of various lengths. These side chains generally have one to three sugars, starting with D-Xyl then D-Gal and L-Fuc; a single-letter nomenclature (X, L, F) corresponding to the last substituted sugar designates each type of side chain (Fry et al., 1993). Successive side chains form specific patterns separated by free Glc residues (G) of the backbone. Biosynthesis of XyGs takes place in the Golgi apparatus and exocytosis delivers the polysaccharides to the cell surface. XyG biosynthesis involves various glycosyl transferases (Lerouxel et al., 2006; Zabotina, 2012). Sugar residues of XyG side chains can also be *O*-acetylated in the Golgi apparatus by *O*-acetyltransferases, but the biological function of acetylation remains unknown (Salisbury et al., 1988). After its delivery to the cell wall, the XyG structure can be modified by xyloglucan endo/transglycosidase hydrolases (XTHs) and glycoside hydrolases (Rose et al., 2002; Harholt et al., 2006). The XTHs exhibit xyloglucan endotransglycosidase and/or xyloglucan endohydrolase (XEH) activities and are responsible for both the integration of newly synthesized XyGs and for polysaccharide remodeling (Rose et al., 2002; Baumann et al., 2007). Xyloglucan biosynthesis and remodeling are proposed to play an important role in growth and development (Fry, 1994; Pauly et al., 2001; Takeda et al., 2002; Ryden et al., 2003; Peña et al., 2004; Swarup et al., 2008). The wall loosening expansins are also important for cell wall restructuring, acting on wall hydration and disrupting hydrogen bonds between XyGs and cellulose microfibrils (Cosgrove, 2000).

Structural variations of XyG chains can alter the properties of the XyG polymer and its cross-linking with cellulose microfibrils, consequently reinforcing or weakening the cell wall (Levy et al., 1997; Cosgrove, 2005; Park and Cosgrove, 2012b; Wolf et al., 2012). A large set of apoplastic glycosidases or *trans*-glycosidases (β-glucosidases, α-xylosidases, β-galactosidases, and α-fucosidases) act specifically on XyGs. These enzymes modify XyG structure by modulating the length of side chains, which might change their susceptibility to XTH activity (Augur et al., 1993; Iglesias et al., 2006; Franková and Fry, 2011) and/or their cellulose binding properties (Levy et al., 1997). Modifications of XyG-cellulose interaction or remodeling of XyG by metabolizing enzymes may modulate cell wall extensibility and thus facilitate cell expansion. Substantial experimental data support a major role of XyG in cell elongation (Cosgrove, 2005; Wolf et al., 2012), but characterization of *Arabidopsis thaliana* mutants altered in XyG structure or even lacking substituted XyG has raised doubts about the critical function of XyGs, as these mutants exhibit no or only subtle phenotypes when grown under standard laboratory conditions (Vanzin et al., 2002; Tamura et al., 2005; Cavalier et al., 2008; Zabotina et al., 2008; Günl et al., 2011). Plant plasticity and compensation mechanisms may account for the lack of apparent phenotypes. Indeed, further studies of the double xyloglucan xylosyltransferase mutant, *xxt1 xxt2*, which lacks substituted XyG, revealed alterations of cellulose organization suggesting more severe alteration of the cell wall than originally reported for these plants (Anderson et al., 2010). Involvement of other matrix components may compensate for XyG structural defects (Park and Cosgrove, 2012a). Further characterization of wild-type and *xxt1 xxt2* cell wall properties provided additional evidence supporting the importance of XyG for primary cell wall strength and wall loosening by expansin A (Park and Cosgrove, 2012a).

In addition, XyG-derived oligosaccharides, also named oligosaccharins, can be released from the cell wall. The modification of XyGs by addition or removal of sugar residues from their side chains affects their biological activity as signaling molecules. In particular, removal of the Fuc from XXFG oligosaccharide fragment suppresses its antiauxin activity (York et al., 1984; Fry et al., 1990).

The effects of auxin on the cell wall extend beyond its interference with oligosaccharins. Apoplastic acidification resulting from auxin-related responses at the plasma membrane is thought to favor the action of expansins on wall loosening (Cosgrove, 2000). Various cell wall–related genes also show differential expression in response to auxin or to alteration of auxin signaling (Lorenzo et al., 2003; Okushima et al., 2005; Overvoorde et al., 2005; Nemhauser et al., 2006; Stepanova et al., 2007; Lewis et al., 2013). However, the effect of such changes in gene expression on the composition or the structure of the cell wall remains unclear.

To further investigate the molecular mechanism by which ABP1 controls cell expansion, we studied transcriptomic changes in dark-grown hypocotyls in response to conditional ABP1 inactivation (Braun et al., 2008) and analyzed the effects on cell wall composition. Here, we report how ABP1 modulates the expression of cell wall related genes and the remodeling of XyG side chain structure, a parameter that turns out to be of critical importance for hypocotyl elongation.

RESULTS

Skotomorphogenesis Requires Functional ABP1

ABP1 acts on cell elongation and cell division in a context-dependent manner and controls a large range of physiological processes (Braun et al., 2008; Tromas et al., 2009). To further investigate the role of ABP1 in cell expansion, we studied the effect of ABP1 inactivation in dark grown seedlings, given that hypocotyl growth in darkness is known to rely solely on enhanced cell elongation (Gendreau et al., 1997). For that purpose, we used transgenic lines (SS12K, SS12S, and AS9.8) that conditionally and functionally inactivate ABP1 upon ethanol induction (Braun et al., 2008). The SS12K and SS12S lines inducibly express the recombinant antibody scFv12, which blocks ABP1 function; the AS9.8 line inducibly expresses an antisense construct targeting *ABP1*. Skotomorphogenesis of wild-type seedlings is characterized by exaggerated elongation of the hypocotyl, maintenance of the apical hook, small closed cotyledons, and reduced root growth

(Figure 1A). By contrast, 4-d-old SS12K seedlings inactivated for ABP1 since germination exhibited a partially deetiolated phenotype with the length of the hypocotyl reduced by more than half compared with the wild type, no apical hook, and open and epinastic cotyledons that remained small. Hypocotyls were also agravitropic (Figure 1A). Similar alterations were observed on independent conditional lines for ABP1 (Supplemental Figure 1), indicating that the partial deetiolation results from the loss of function of ABP1. To determine whether the shorter hypocotyls resulted from an early arrest of growth or from a reduced elongation rate, we measured hypocotyl elongation of dark-grown seedlings over 10 d (Figure 1B). Hypocotyl elongation kinetics revealed a defect in hypocotyl growth from the early stages of development of ABP1 inactivated seedlings. In addition, the hypocotyl length plateaued at least 2 d before the maximal elongation in wild-type seedlings, indicating that ABP1 inactivation also reduces the period of growth.

To further investigate the difference in hypocotyl growth between wild-type and ABP1 inactivated seedlings, we measured the length of individual epidermal cells along the full length of dark-grown hypocotyls of ethanol induced seedlings for both genotypes after 48, 72, and 96 h of culture (Figure 1C). The overall size of SS12K epidermal cells was reduced compared with the wild type. However, elongation defects were not equally distributed along the hypocotyl. In our experimental growth conditions, at 48 h, wild-type epidermal cells 1 to 12, numbered from the base of the hypocotyl, underwent huge elongation with cells 5 and 6 undergoing maximum elongation to around 600 µm. At 48 h, ABP1 inactivation inhibited the elongation of basal cells; cells 5 and 6 were 2.7-fold smaller than in the wild type. The maximal elongation in SS12K shifted to cells 9 to 11, with their length being reduced by 40% compared with the same rank of cells in the wild type. At later stages, the elongation zone moved up for both genotypes and the 40% decrease of cell length was maintained from the middle to the top of the hypocotyl. To visualize the elongation zone, we also used the marker pCESA6:GUS (for β-glucuronidase), which expresses only in expanding tissue (Desprez et al., 2007). GUS staining confirmed the progression of the elongation zone from the base of the hypocotyl to the upper part over time (Figure 1D). We observed no significant change in the organization of hypocotyl cell files and no change in radial expansion (Figure 1E).

We thus measured the thickness of the external epidermal cell wall at the base and in the elongation zone of hypocotyls. Both genotypes had thinner cell walls at the base of the hypocotyl, where cells have achieved their full elongation and started to differentiate compared with the elongation zone (Figures 1F and 1G). At both positions, the cell wall was significantly thicker in hypocotyls inactivated for ABP1, reflecting the overall reduced cell elongation and suggesting that synthesis or deposition of cell wall material remained unaffected.

ABP1 Affects Expression of Cell Wall Genes in Dark-Grown Seedlings

To further understand the involvement of ABP1 in the control of hypocotyl growth in darkness, we performed a transcriptomic analysis to provide an overview of the biological processes that are disturbed after inactivation of ABP1. We compared gene expression of SS12K dark-grown seedlings inactivated for ABP1 either since germination (96 h) or for a short time (8 h of exposure to the inducer) to the respective control seedlings (plants expressing GUS under the same ethanol inducible system). Considering the minimal time required after ethanol induction for production of scFv12 recombinant antibodies, 8 h of induction corresponds to an average of 2 h of effective functional inactivation of ABP1. Statistical analysis was performed using a combination of 2-fold change on the mean of the biological replicates and false discovery rate below 0.05. Remarkably, many genes exhibited differential expression following ABP1 inactivation in both cases, confirming the broad and critical importance of ABP1 (Figure 2A). Even after 8 h of ethanol induction, 1185 genes exhibited differential expression, almost equally distributed between induced and repressed genes. About half of the upregulated genes are consistently upregulated over time, as they are common between short and long term inactivation samples. Other long-term upregulated genes (1168) likely result from indirect processes, including many related to plastid differentiation (Supplemental Figure 2). Interestingly, based on gene ontology classifications, cell wall–related genes are overrepresented among up- and downregulated genes in short- and long-term ABP1 inactivation by more than 2-fold compared with random draw (Figure 2B; Supplemental Figure 2 and Supplemental Data Set 1). To have a more comprehensive view of cell wall–related processes, the list of annotated cell wall related genes in TAIR was supplemented with up to 989 genes whose expression relates to cell wall biogenesis (Jamet et al., 2009). As a result, a set of 217 cell wall genes was thus recorded as differentially expressed upon ABP1 inactivation. ABP1 inactivation caused major changes in the expression of genes involved in cell wall remodeling but affected few genes involved in cell wall biosynthesis (Figure 2C). Genes involved in hemicellulose modifications, such as glycosyl hydrolases or different classes of XTHs, were among the most differentially affected by the loss of function of ABP1. ABP1 inactivation also affected expansins A, which promote cell wall loosening in response to acidification (Cosgrove, 2000). In summary, differential expression of cell wall–related genes suggests a role of ABP1 in the modulation of cell wall extensibility to sustain cell expansion.

The transcriptomic analysis was designed to avoid possible interference with ethanol treatment as both genotypes were exposed to ethanol vapors in identical conditions. However, we used a subset of cell wall–related genes belonging to various gene families and exhibiting differences between the wild type and SS12K to verify that ethanol treatment has no effect on their expression in the wild-type background (Supplemental Figure 3).

We took advantage of previously released transcriptomic data on deetiolated seedlings to perform meta-analysis. Data from paclobutrazol-induced (an inhibitor of gibberellin [GA] biosynthesis) deetiolated seedlings and the *det2* mutant were compared with long ABP1 inactivation to determine the possible influence of ABP1 knockdown on GA and/or brassinosteroid pathways, respectively (Gallego-Bartolomé et al., 2012). A limited number of genes was found to be in common between ABP1 inactivation and paclobutrazol-treated seedlings or *det2* mutants (Supplemental Figure 4A). Among cell wall–related genes affected after inactivation of ABP1, only 12 and 27 genes were found to be differentially

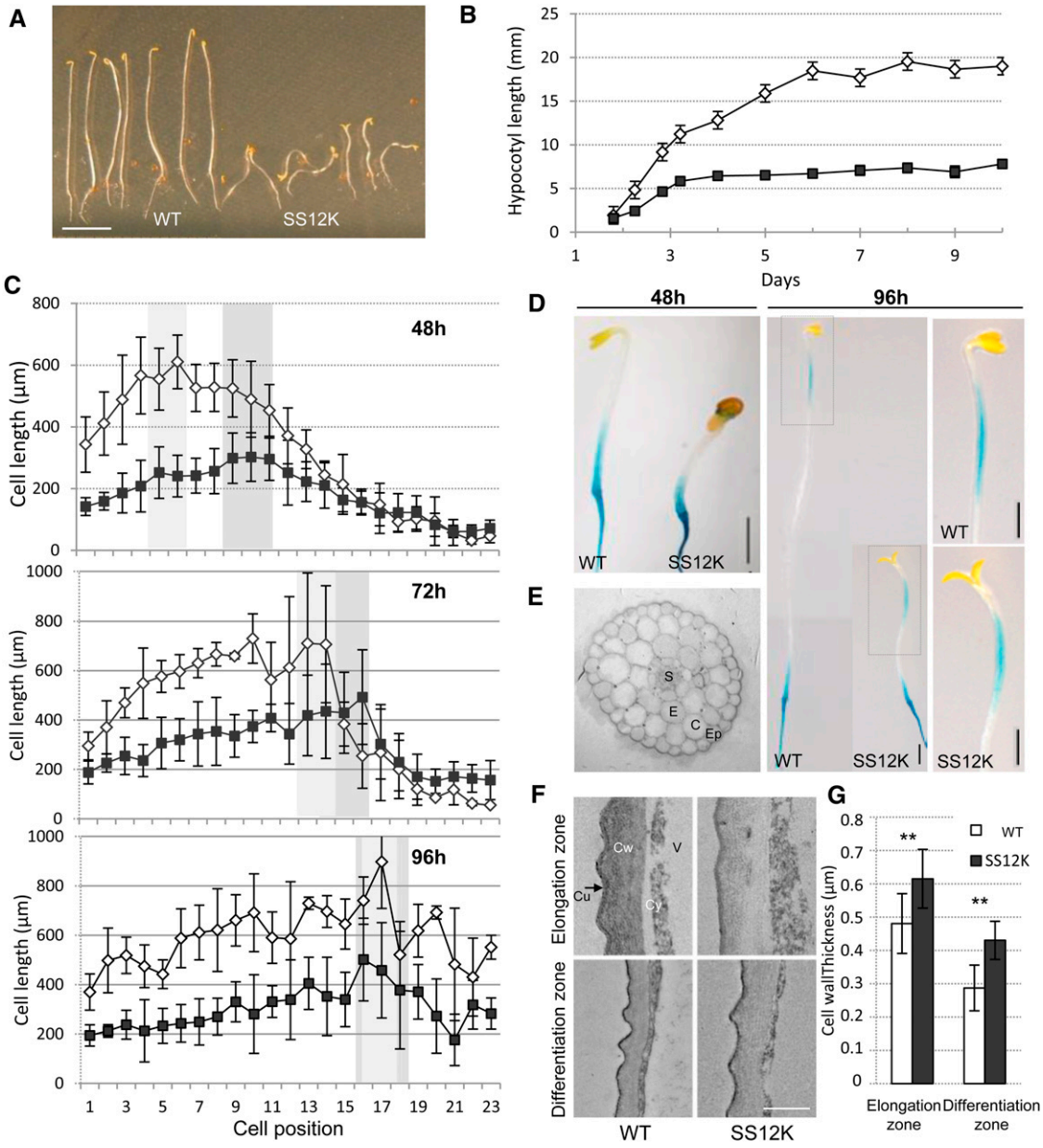

Figure 1. Characterization of the ABP1 Loss-of-Function Phenotype.

(A) Dark-grown phenotype of seedlings of the wild type (left) and SS12K inactivated for ABP1 since germination (right). Bar = 5 mm.
(B) Kinetics of hypocotyl elongation of ethanol-induced wild-type and SS12K dark-grown seedlings. Data represent mean ± SD (n = 25)
(C) Length of hypocotyl epidermal cells in individual cell files along ethanol-induced wild-type and SS12K dark-grown seedlings at 48, 72, and 96 h from base to apex. Error bars represent SD (n = 8 files from six or seven hypocotyls for SS12K; n = 3 files from three wild-type hypocotyls). Light- and medium-gray backgrounds underline cell elongation maxima in the wild-type and SS12K, respectively.
(D) Elongation zone visualized by expression of *pCESA6:GUS* in ethanol-induced wild-type and SS12K of 2- and 4-d-old dark grown seedlings. Close-up photos on the right correspond to the dotted line frames at 96 h. Bars = 1 mm.
(E) Cross sections of 3-d-old dark-grown hypocotyls of SS12K. Ep, epidermis; C, cortical cells; E, endodermis; S, stele
(F) Ultrathin transverse section of external epidermal cell wall of wild-type and SS12K dark-grown hypocotyls. Sections were taken at the elongation zone and at the base of 3-d-old hypocotyls. Cu, cuticle; Cy, cytoplasm; Cw, cell wall; V, vacuole. Bar = 500 nm.
(G) Cell wall thickness of external epidermal wall as in **(F)**. Data are mean ± SD. Measurements were performed on 16 to 19 cells from three hypocotyls for each. **P value < 0.001.

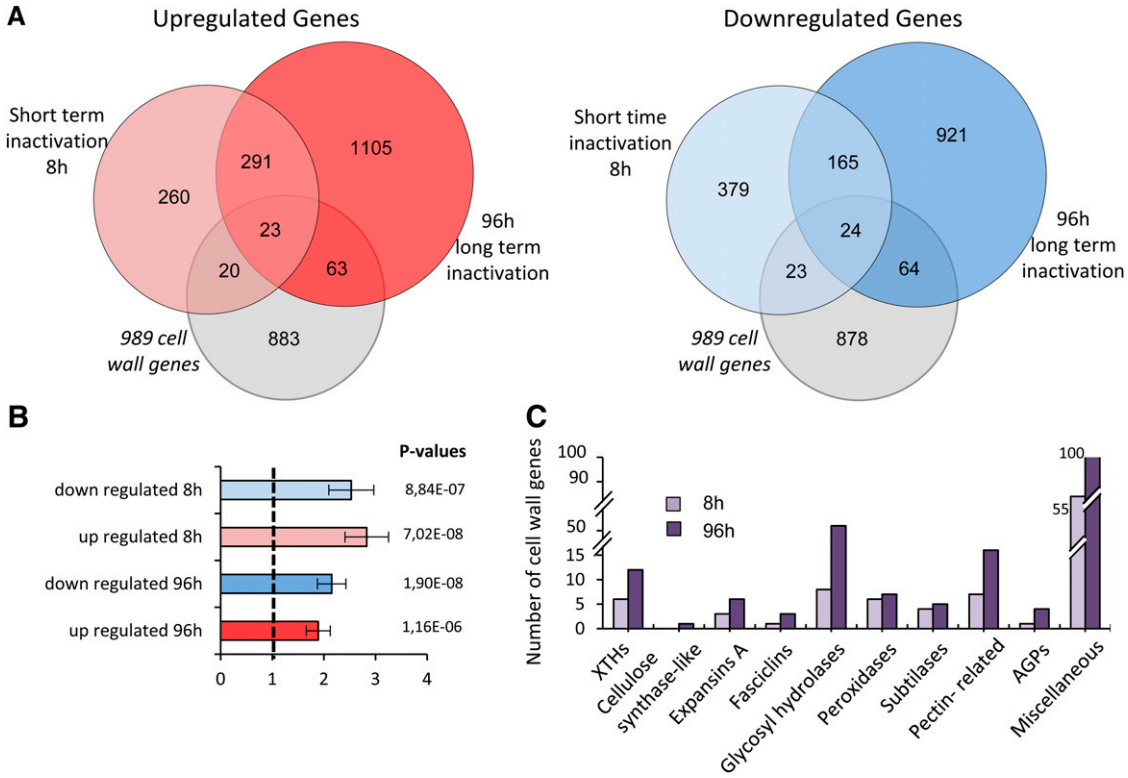

Figure 2. Comparative Analysis of Genes Differentially Expressed between ABP1-Inactivated and Control Dark-Grown Seedlings after Short- and Long-Term Ethanol Induction.

Ethanol induction results in ABP1 inactivation in SS12K and expression of GUS reporter in the control line

(A) Venn diagram representing the number of overlapping and unique upregulated (left) and downregulated (right) genes after 8 and 96 h of ethanol induction promoting scFv12 expression and resulting inactivation of ABP1. Differentially expressed genes are also compared with cell wall annotated genes (gray circle) in TAIR10 implemented by cell wall genes expressed in dark-grown hypocotyl listed by Jamet et al. (2009).

(B) Histograms illustrating the overrepresentation of cell wall–related genes after inactivation of ABP1. The data take into account normalization to the total number of cell wall genes present on the chip.

(C) Major classes of cell wall genes differentially expressed after short- and long-term inactivation of ABP1.

expressed in paclobutrazol-treated and *det2* seedlings, respectively (Supplemental Figure 4B and Supplemental Data Set 2). Similarly we compared the transcriptomic data obtained on dark-grown *cop1-4* seedlings, which are impaired in the master repressor of photomorphogenesis COP1 (Ma et al., 2002). We found 162 genes in common with long ABP1 inactivation, among which only 19 were cell wall–related genes (Supplemental Figures 4C and 4D and Supplemental Data Set 2). In conclusion, deetiolation induced by GA deficiency (paclobutrazol treatment), BR deficiency (*det2* mutation), or *cop1-4* mutation does not cause the same changes in gene expression, including cell wall genes, as those induced by ABP1 knockdown. ABP1 inactivation generates a specific profile of gene expression with unique overrepresentation of cell wall–related genes. This finding motivated us to analyze cell wall composition and structure in ABP1 knockdown.

ABP1 Affects Xyloglucan Structure

To evaluate the consequences of the differential expression of cell wall–related genes on cell walls, we analyzed the composition of wall polysaccharides after inactivation of ABP1. We first quantified the composition in monosaccharides (Figures 3A and 3B), which revealed that cell walls of ABP1 inactivated dark-grown seedlings have less Xyl, cellulosic Glc, and uronic acid. A tremendous increase in noncellulosic Glc was observed in SS12K. Lugol staining revealed that deetiolated SS12K seedlings accumulate large amount of starch in cotyledons (Figure 3C), which can account for the difference in noncellulosic Glc (Figure 3A). Comparison by Lugol staining of the *cop10.4* mutant, which exhibits a similar deetiolation phenotype to SS12K (i.e., cotyledon opening, absence of apical hook, and similar reduction of hypocotyl lengthening), revealed that starch accumulation is not shared by all deetiolated mutants (Supplemental Figures 5A to 5C). Next, we performed a glycosidic linkage analysis (Figure 3D). The increase in 1,4-Glc probably reflects the presence of starch in the alcohol insoluble fraction. More critically, 1,2-Xyl, which is specific to XyG (Zablackis et al., 1996), was reduced as well as 1,4,6-Glc, despite the increase of starch content in the mutant. The decrease in the relative content of t-Xyl and 1,2-Xyl confirmed the global reduction of Xyl monosaccharide in the composition analysis.

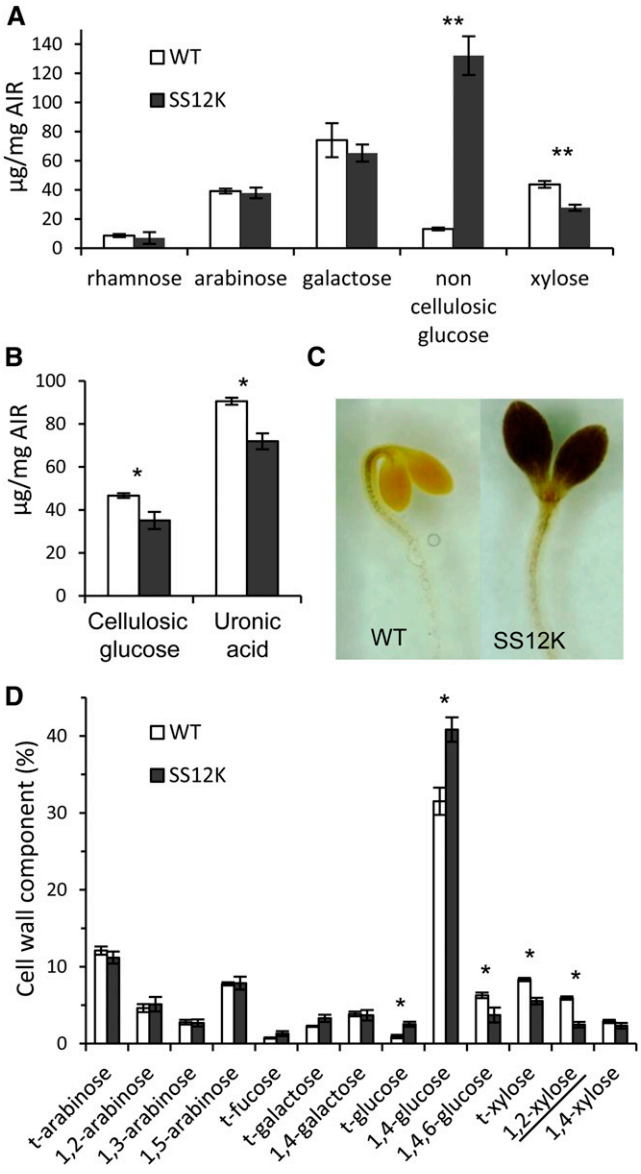

Figure 3. Cell Wall Analyses of Wild-Type and SS12K Dark-Grown Seedlings

(A) Monosaccharide composition analysis of the wild type and SS12K. AIR, alcohol-insoluble residue. Bars represent SD (n = 4 biological replicates); **P value < 0.001.

(B) Quantification of cellulosic Glc and uronic acid. Bars represent SD (n = 4 biological replicates); *P value < 0.05.

(C) Lugol staining of wild-type and SS12K dark-grown seedlings.

(D) Glycosidic linkage analysis of cell wall polysaccharides extracted from ethanol-induced wild-type and SS12K dark-grown hypocotyls. Data are mean ± SD (n = 4 biological replicates); *P value < 0.01

To further characterize XyG structure in hypocotyls inactivated for ABP1, we used oligosaccharide mass profiling (OLIMP) (Lerouxel et al., 2002). XyG fragments were generated by endo-(1→4)-β-glucanase enzymatic digestion, which cleaves the XyG backbone after nonsubstituted Glc. The mass spectrometry provides relative abundance of the released oligosaccharide XyG from the polymers, which gives information about the structure of the XyG. Functional inactivation of ABP1 resulted in robust changes in the relative abundance of specific XyG fragments (Figure 4; Supplemental Figure 6). In particular, XXXG and XXLG/XLXG decreased, whereas *O*-acetylated XXLG and especially *O*-Ac-XXFG increased. More complex fragments also significantly increased as an uncharacterized 1541 *m/z* ion that is consistent with being Hex_7Pent_2 (Hsieh and Harris, 2012). The biological function of cell wall polymer *O*-acetylation is still unclear, and the relative ratio varies to some extent; however, the sum of non-acetylated and *O*-acetylated XXFG always increased after ABP1 inactivation, revealing that XyGs were enriched in long and fucosylated side chains (Figure 4D). Other fucosylated OXyGs, such as XFLG and its acetylated form, were either not found or only found as traces on both genotypes. Considering our analysis of cell wall polysaccharides, the observed alterations resulting from inactivation of ABP1 appear to be specific to XyG and more precisely to modifications of XyG side chain composition. To explore whether alteration of the auxin binding capacity of ABP1 would result in similar changes in XyG, we grew *abp1-5* mutants in darkness and analyzed XyG structure. The *abp1-5* point mutation affects one of the residues of the auxin binding pocket and was hypothesized to impair the binding of auxin to the protein (Robert et al., 2010; Xu et al., 2010). The phenotype of the mutant and the relative distribution of XyG fragments were similar to control seedlings (Figure 5), indicating that growth defects and the alteration of the XyG structure result from the knockdown of ABP1 protein rather than impaired binding of auxin to the protein.

Importantly, the XyG analysis of the *cop10-4* mutant (Supplemental Figures 5D and 5E) did not mimic the alterations observed in ABP1 inactivated seedlings, indicating that these XyG changes are not a common feature of deetiolated mutants but are specific consequences of the loss of ABP1 function.

Modulation of Xyloglucan Fucosylation in Muro Restores Hypocotyl Elongation

We then addressed the question of the relative importance of XyG fucosylation in the reduced cell expansion in ABP1 inactivated hypocotyls. To manipulate XyG fucosylation in ABP1 knockdown seedlings, we took advantage of previously reported plants that are either defective for the Golgi-located FUT1/MUR2 fucosyl transferase, responsible for XyG fucosylation during biosynthesis (Vanzin et al., 2002), or overexpress the apoplastic *FUC95A* fucosidase (*35S:AXY8*) promoting XyG defucosylation in muro (Günl et al., 2011). The conditional construct for ABP1 was introgressed by crossing into the *mur2-1* mutant, which is null for the fucosyl transferase FUT1/MUR2 and into *35S:AXY8* transformants. In accordance with previous work (Vanzin et al., 2002), *mur2-1* mutant exhibited a drastic decrease in fucosylated XyG fragments and a reciprocal increase of XXLG/XLXG polymers (Figure 6A). A similar profile was observed in the SS12K background; however, a slight and significant increase of XXFG, *O*-acetylated XXLG, and XXFG as well as the increase of the 1541 *m/z* ion were observed after inactivation of ABP1. Similarly, overexpression of the fucosidase promoted partial defucosylation of XyGs (Figure 6B). Interestingly, the *mur2* mutation did not

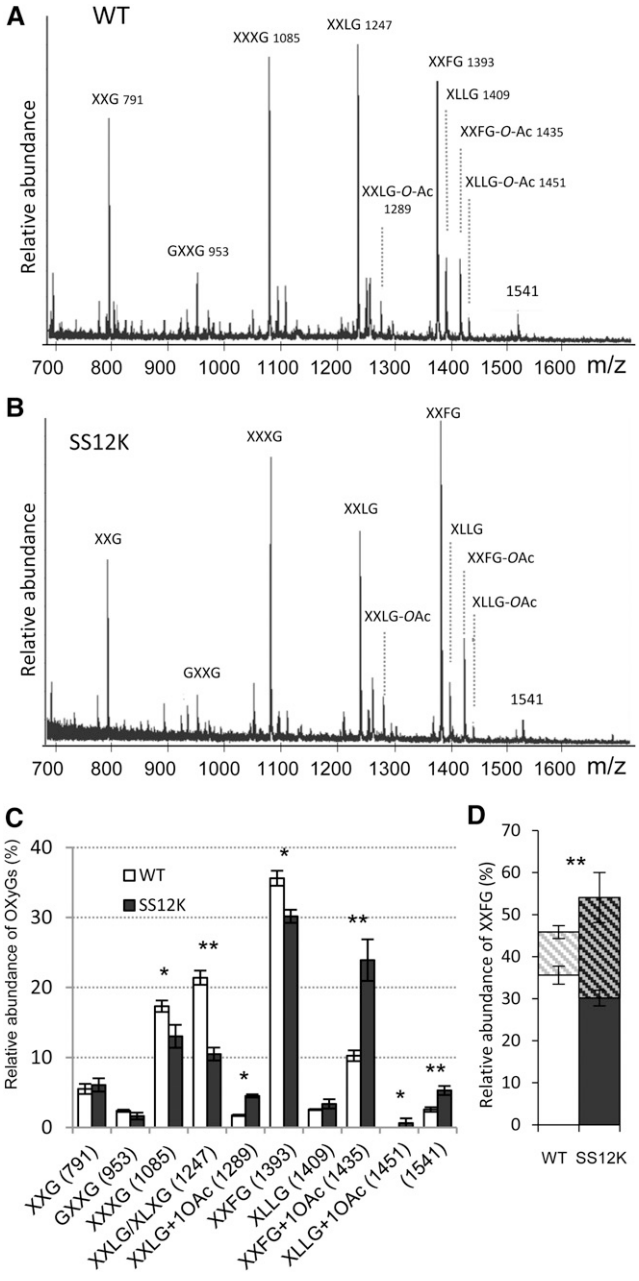

Figure 4. Xyloglucan Fingerprinting of Dark-Grown Hypocotyls

(A) and **(B)** Representative spectra of oligosaccharides released by the endoglucanase and analyzed by OLIMP of ethanol-induced wild-type **(A)** and SS12K **(B)** 4-d-old dark-grown hypocotyls.

(C) Quantitative analysis of OLIMP data for the wild type and SS12K. Data are mean ± SD (n = 4 biological replicates). *P < 0.05 and **P < 0.01

(D) Relative amount of fucosylated OXyG fragments in the wild type and SS12K. Histograms represent the sum of *O*-acetylated and non-acetylated XXFG for each genotype. **P value < 0.01

result in significant change in the ABP1 knockdown phenotype, whereas defucosylation mediated by AXY8 at the cell wall partially restored hypocotyl elongation (Figures 6C and 6D). Hypocotyl length of dark-grown *35S:AXY8*,SS12K seedlings was twice the length of SS12K, whereas agravitropic defect and cotyledon opening were still as in SS12K. These observations suggest that cell wall fucosidase activity was defective in ABP1 loss of function, thus impairing the capacity of the hypocotyl cells to expand. While *AXY8* expression was downregulated after inactivation of ABP1, conversely, introgression of *35S:AXY8* construct promoted elevated overexpression in both genotypes (Figure 6E).

The production of XyGs with shorter side chains is not sufficient to modify the elongation of hypocotyls inactivated for ABP1 whereas an in muro modification of XyG fucosylation during the elongation process restores hypocotyl growth. These data point to the critical importance of the length and composition of XyG

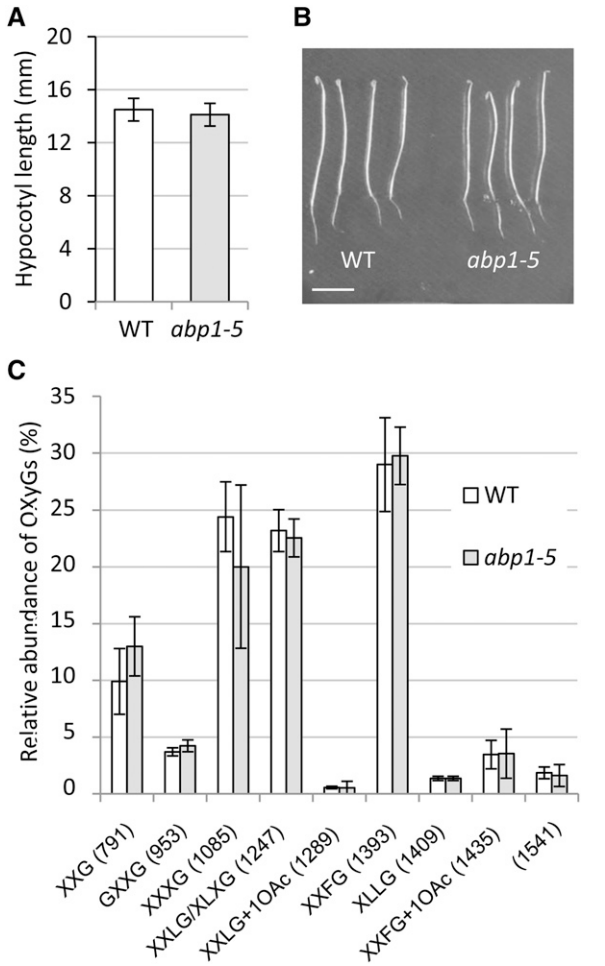

Figure 5. Xyloglucan Fingerprinting of Dark-Grown *abp1-5* Hypocotyls.

(A) Hypocotyl length of 4-d-old dark-grown seedlings

(B) Phenotypes of dark-grown seedlings

(C) Quantitative analysis of OLIMP data for the wild type and *abp1-5*. Data are mean ± SD (biological replicates n = 4). None of the differences are statistically significant.

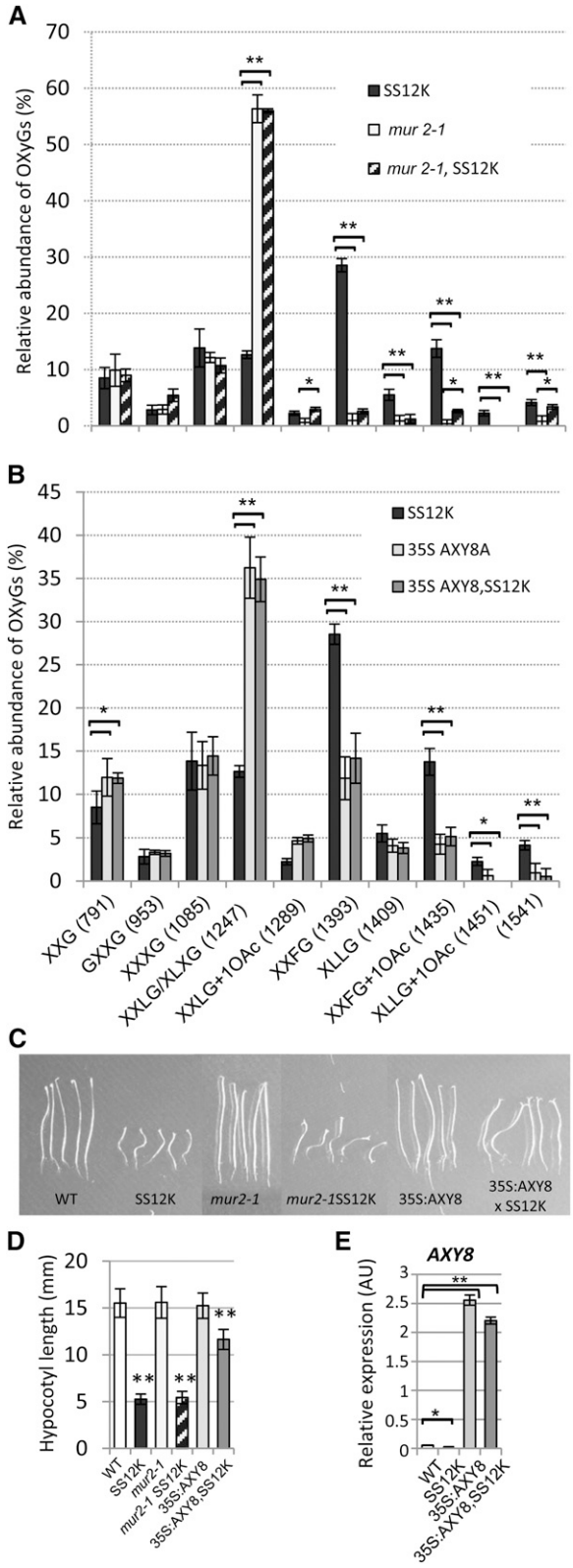

Figure 6. Partial Restoration of Cell Expansion in ABP1-Inactivated Hypocotyls of SS12K by α-Fucosidase–Mediated Xyloglucan Defucosylation.

side chains for cell expansion, with major differences between biosynthesis and modifications occurring later within the cell wall.

ABP1 Acts on Xyloglucan Structure through Modulation of Gene Regulation Mainly via Its Effect on the SCF$^{TIR1/AFBs}$ Pathway

We recently demonstrated the modulation of the SCF$^{TIR1/AFBs}$ pathway by ABP1 (Tromas et al., 2013). In particular, we reported that multiple null mutations in *TIR1* and *AFBs* suppress the severe developmental alterations of light-grown ABP1-inactivated seedlings. Here, we took advantage of this genetic material to investigate whether ABP1-dependent alterations of XyGs result from the activity of the protein at the plasma membrane or from the control exerted by ABP1 on the TIR1/AFB-AUX/IAA pathway. This question deserved to be raised especially considering the partial restoration of hypocotyl growth after *AXY8* overexpression and the resulting remodeling of XyG. We first checked whether *tir1/afb* mutations suppress the deetiolated phenotype of dark-grown SS12K seedlings. Inactivation of ABP1 in the *tir1-1 afb2-1 afb3-1* background did not result in the deetiolated phenotype, indicating that it requires the TIR1/AFB-AUX/IAA pathway (Figure 7A). Cotyledon opening and hypocotyl elongation were all restored, in contrast with the partial restoration of hypocotyl elongation observed after *AXY8* overexpression. Irrespective of the functionality of ABP1, the hypocotyl length of the triple *tir1/afb* mutant was 20% shorter than that of the wild type and the apical hook was less pronounced (Figures 7A and 7B). The suppression of the ABP1 inactivation phenotype by *TIR1/AFB* mutations while ABP1 is still inactive offered a unique opportunity to discriminate between genomic and nongenomic dependent role of ABP1 on cell wall composition. We focused on XyG fragments exhibiting consistent differences between the wild type and lines inactivated for ABP1. Analysis of the triple mutant *tir1-1 afb2-1 afb3-1* with or

(A) Comparison of the relative abundance of a selection of OXyGs, quantified from OLIMP spectra, between ethanol-induced hypocotyls of SS12K, *mur2-1* null mutant, and SS12K in *mur2-1* background. Statistical tests were calculated for SS12K versus *mur2-1* or versus *mur2-1*SS12K; *mur2-1* was also compared with *mur2-1*SS12K. *P < 0.05 and **P < 0.005.

(B) Comparison of the relative abundance of a selection of OXyGs, quantified from OLIMP spectra, between ethanol-induced hypocotyls of SS12K, 35S:AXY8 overexpressor, and SS12K 35S:AXY8 double transformants. In **(A)** and **(B)**, data are mean ± SD (biological repeats $n = 4$). Statistical tests were calculated for SS12K versus 35S:AXY8 or 35SAX8, SS12K. *P < 0.05 and **P < 0.001.

(C) Phenotype of 4-d-old dark-grown seedlings. Statistical tests were calculated by comparing each genotype with and without SS12K. **P < 0.001.

(D) Hypocotyl length of 4-d-old dark-grown seedlings. Bars represent SD ($n = 4 \times 25$).

(E) mRNA accumulation of *AXY8* in dark-grown seedlings exposed to ethanol vapors since germination. Data were normalized with respect to *ACTIN2-8* and expressed in relative units. Bars represent SD (three biological repeats and two technical replicates). Statistical tests were calculated by comparing the wild type to other genotypes. *P < 0.05 and **P < 0.001. AU, Actin unit.

without inactivation of ABP1 revealed an OXyG profile very similar to the wild type (Figure 7C). Loss of function for up to three members of the TIR1/AFB F-box family had no measurable effect on XyG structure but paradoxically was sufficient to suppress cell wall defects resulting from ABP1 inactivation. These data lead to the conclusion that observed alterations in XyGs in ABP1-inactivated dark-grown seedlings reflect the effect of ABP1 on the $SCF^{TIR1/AFB}$ pathway.

We thus analyzed whether *tir1/afb* mutations fully restored the steady state expression of cell wall–related genes found to be altered after ABP1 inactivation. In the context of this study, we mainly focused on genes involved in XyG modifications (Figure 7D; Supplemental Figure 7). Figure 7D is a selection of representative genes exhibiting distinct steady state expression after alteration of the ABP1 and/or the $SCF^{TIR1/AFB}$ pathways. Importantly, real-time RT-PCR analyses mainly confirmed ABP1-dependent differential

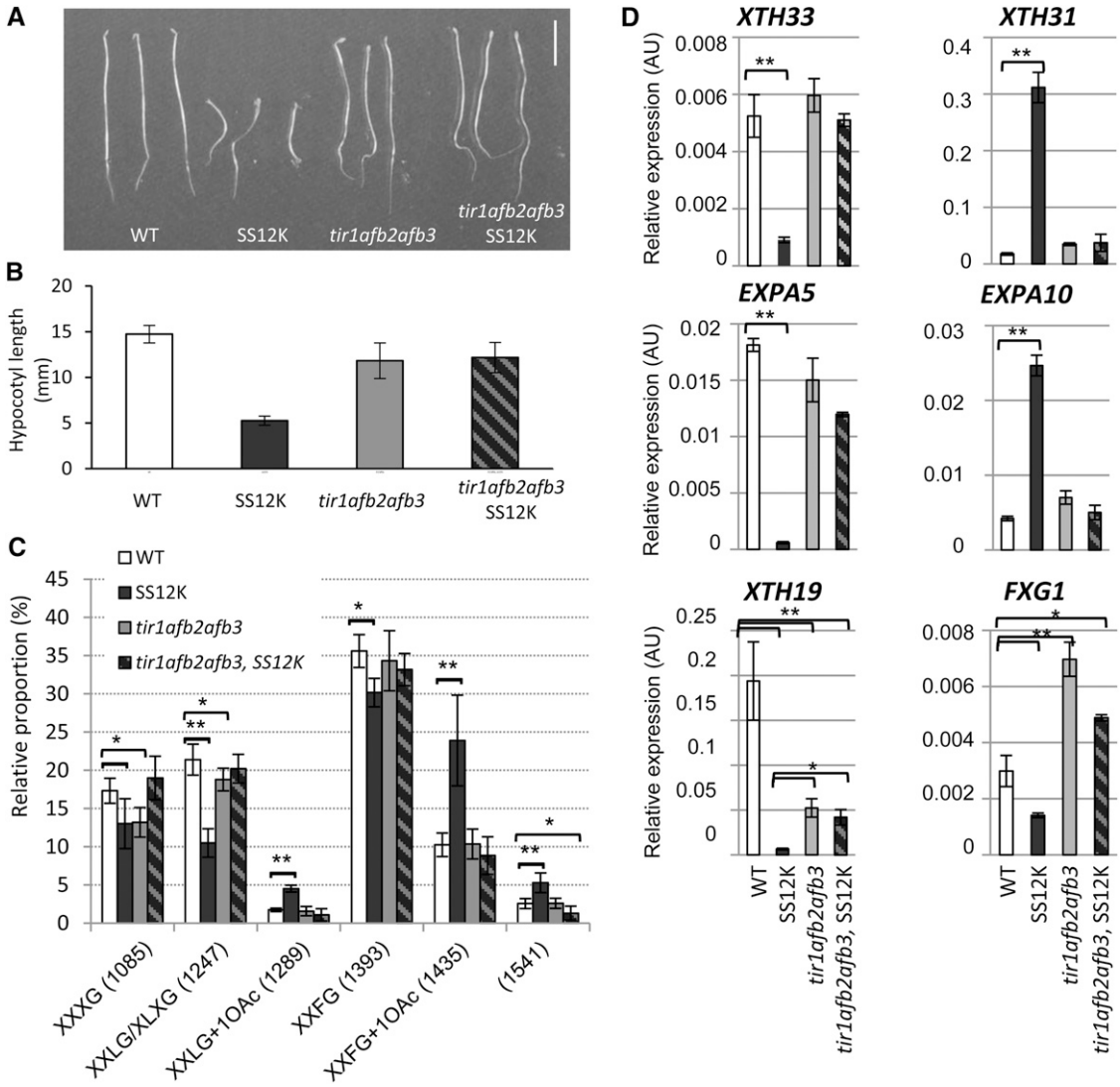

Figure 7. Suppression of ABP1 Loss-of-Function Phenotype in SS12K *tir/afbs* Background.

(A) Phenotype of 4-d-old dark-grown seedlings as indicated.

(B) Hypocotyl length for 4-d-old dark-grown seedlings.

(C) Comparison of the relative abundance of a selection of OXyGs, quantified from OLIMP spectra, between ethanol-induced hypocotyls of the wild type, SS12K, *tir1-1 afb2-1 afb3-1* triple mutant, and SS12K in the triple F-box mutant background. Data are mean ± SD (biological repeats $n = 4$). Statistical tests were calculated for the wild type versus each other genotypes. *P < 0.02 and **P < 0.001.

(D) RNA accumulation of a selection of XyG-related genes in the distinct genotypes as indicated. All data were normalized with respect to *ACTIN2-8* and expressed in relative units. For all graphs, data are mean ± SD (biological repeats $n = 3$, and two technical repeats for each). Differences between the wild type and SS12K are always significant at P value < 0.01. The wild type versus *tir1 afb2 afb3* or *tir1 afb2 afb3* SS12K is as indicated (*P < 0.05 and **P < 0.01). AU, Actin unit.

expression identified from the transcriptomic data. Within the same gene family and even the same subfamily, opposite effects of ABP1 inactivation were observed, as for *XTH33* or *EXPA5* and *XTH31* or *EXPA10*, which were down- and upregulated, respectively. No or weak modification of expression was detected for these genes in the triple *tir1-1 afb2-1 afb3-1* mutant and in this background, inactivation of ABP1 no longer had any effect on the accumulation of their transcripts. *XTH18* illustrates genes that were downregulated in ABP1-inactivated seedlings as well as in the triple *tir1/afbs* mutant, the combination of both being very similar to the triple mutant. Finally, the putative XyG α-fucosidase *FXG1* was found to be downregulated after inactivation of ABP1 (as observed above for *AXY8*; Figure 6E), upregulated in the triple mutant, and to be intermediate in the combination of both. In most cases, *tir1/afb* mutations restored the expression of genes altered after ABP1 inactivation either to a wild-type level or to the level of the mutant, confirming that ABP1 mainly acts through the $SCF^{TIR1/AFB}$ pathway. Analysis of expression of these genes after treatment of wild-type-dark grown seedlings with 10 μM IAA was also performed (Supplemental Figure 8). Most of the genes that were downregulated in seedlings inactivated for ABP1 and in the triple *tir/afb* mutant exhibited weak or transient increased accumulation of their mRNA, with potentially distinct kinetics, in response to auxin as *XTH18*, *XTH19*, or *EXPA4*. Genes that were upregulated after ABP1 inactivation and not significantly affected in the triple mutant, such as *XTH31* or *EXPA10*, were not found to be responsive to auxin in our experimental conditions. Finally, genes that were downregulated after ABP1 inactivation, such as *XTH33* and *FXG1*, and were not affected or induced in the triple mutant, were induced or slightly decreased, respectively, thus revealing a complex network of gene regulation.

DISCUSSION

ABP1 Is Essential for Control of Cell Wall–Related Gene Expression

The plant-specific protein ABP1 functions in auxin-dependent processes, but remains enigmatic despite recent progress. Null mutation and induced loss of function for ABP1 result in severe and pleiotropic defects of *Arabidopsis* growth and development with *abp1-2* null mutant being embryo lethal and conditional plants exhibiting a large range of alterations at all stages of development (Chen et al., 2001; Braun et al., 2008; Tromas et al., 2009; Xu et al., 2010). These broad effects result from the action of ABP1 on cell division (David et al., 2007; Tromas et al., 2009) and also its requirement for cell expansion in shoot tissues (Braun et al., 2008; Xu et al., 2010). Conversely, the *abp1-5* mutation, which affects the auxin binding pocket and was proposed to impair the binding of auxin to the protein (Robert et al., 2010; Xu et al., 2010), results in only very subtle phenotypes, reinforcing the idea that in addition to responses triggered by auxin binding, the protein plays a critical and constitutive role. Moreover, ABP1 is involved in both rapid and nongenomic responses to auxin and in the regulation of gene expression, at least for a subset of early auxin response genes (Braun et al., 2008; Tromas et al., 2009; Effendi et al., 2011). The microarray data generated on dark-grown seedlings reveal that functional inactivation of ABP1 affects the expression of a large number of genes, even after a short-term inactivation of the protein, consistent with the pleiotropism and severity of observed phenotypes (Figure 1). Genes altered in ABP1 loss-of-function plants encompass many cell wall related genes encoding structural cell wall proteins and enzymes involved in cell wall modifications or remodeling (Figure 2; Supplemental Data Set 1). Interestingly, the regulation of these particular genes seems to be a specific molecular feature caused by the inactivation of ABP1 and unconnected to its deetiolated phenotype, since it is not shared with other mutants that also deetiolate in darkness (Supplemental Figure 5). Genes encoding glycosyl hydrolases, XTHs, and A-type expansins were among the most affected. Within these families, most genes were repressed, indicating that functional ABP1 is required to support their expression during hypocotyl growth. Genes of a majority of XTH that were reported to have xyloglucan endotransglycosidase activity are repressed, as well as genes encoding XyG α-fucosidases (*FXG1* and to a lesser extent *AXY8*) and β-galactosidases (Figure 7; Supplemental Figure 7). All these enzymes, as well as expansins, act on XyG remodeling or XyG-cellulose cross-links, and the concomitant decrease of their relative expression is likely to affect primary wall extension. Interestingly, *XTH31* and to a lesser extent *XTH32*, which belong to the group III-A of *XTH* genes, were expressed at a higher level after inactivation of ABP1. These enzymes were reported to be responsible for most of the hydrolysis of xylosylated or galactosylated xyloglucans occurring in parallel with primary wall expansion and were proposed to have integral roles in xyloglucan assembly or disassembly (Baumann et al., 2007; Maris et al., 2011).

ABP1 Acts Mainly via the $SCF^{TIR1/AFB}$ Pathway

Suppression of the developmental alterations resulting from ABP1 inactivation by loss-of-function mutations in *TIR1* and *AFB* F-box genes suggests that modifications of gene expression via the $SCF^{TIR1/AFB}$ pathway are predominantly responsible for the restoration of the dark-grown phenotype. This restoration of gene expression includes several cell wall genes irrespective of whether their expression was repressed or induced after ABP1 inactivation (Figure 7D; Supplemental Figure 7). However, the variety of expression profiles indicates that ABP1-dependent gene expression is not only dependent upon the $SCF^{TIR1/AFB}$ pathway. The genes that are up- or downregulated after ABP1 inactivation but unchanged in the triple mutant show a complete restoration of expression. That is the case for *XTH33*, *XTH31*, *EXPA5*, *EXPA10*, and several others (Figure 7D; Supplemental Figure 7) for which null mutations in *TIR1* and *AFBs* do not impair their expression but are sufficient to restore expression when ABP1 is not functional. For genes that are impaired in the triple *tir1/afbs* mutant, there is an apparent partial restoration close to the level of expression in the triple mutant. For example, this is the case for *XTH19*, which is repressed in both SS12K and the triple *tir1/afbs* mutant. This gene was also induced by auxin, as previously reported (Vissenberg et al., 2005). Its downregulation in all genotypes suggests that both ABP1 and TIR1/AFB pathways are required. Conversely, cell wall genes that were already reported as auxin-regulated genes in etiolated hypocotyls were not

differentially expressed in SS12K, as in *EXPA1*, for example (Esmon et al., 2006). A simple and unique model of $SCF^{TIR1/AFB}$-dependent gene regulation is clearly not sufficient to account for the complexity of the distinct expression profiles found in the different genetic backgrounds. Previous transcriptomic analyses comparing gene expression in auxin signaling mutants or after auxin treatments have already reported important changes in cell wall related genes (Pufky et al., 2003; Okushima et al., 2005; Overvoorde et al., 2005; Nemhauser et al., 2006; Lewis et al., 2013). The correlation between the auxin-mediated regulation, including cell wall genes, and alteration of their expression in *axr3-1* (Overvoorde et al., 2005) or *nph4-1 arf19-1* (Okushima et al., 2005) auxin signaling mutants was paradoxically not so well established. We observed similar discrepancies when comparing effects of ABP1 inactivation, mutations in TIR1, AFB2, and AFB3, and auxin treatment, which is likely to reflect a rather predictable involvement of multiple transcriptional factors acting in combination to control gene expression and/or feedback regulatory loop buffering transcriptional responses. In any case, it appears that an ABP1-dependent pathway massively affects gene expression, sometimes in concert with the $SCF^{TIR1/AFB}$ pathway, sometimes exerting opposite effects.

Interestingly, whereas gene expression and the dark-grown phenotype of *tir1 afb2 afb3* SS12K are similar to those of the class III *tir1 afb2 afb3* mutant (Dharmasiri et al., 2005) (Figures 7A and 7B), its XyG structure is fully restored as in wild-type hypocotyls (Figure 7C). This suggests that gene alterations that are still observed in the triple mutant are not critical for XyG structure. In these seedlings with restored hypocotyl elongation, ABP1 is still inactivated, thus indicating that the protein does not have a critical role on cell wall acidification and related cell wall loosening independently of its transcriptional role, as originally hypothesized.

ABP1 Affects Xyloglucan Structure

Considering the relatively large number of cell wall–related genes differentially expressed after inactivation of ABP1, it was somewhat surprising that no massive changes in the cell wall composition were observed. Cell wall changes essentially concerned XyG and more specifically the length of side chains that were globally enriched into Fuc and *O*-acetylation.

Arabidopsis mutants null for the α-fucosidase AXY8 exhibit increased XyG fucosylation, but these changes in XyG structure were not associated with significant growth or developmental phenotypes (Günl et al., 2011). Similarly, growth defects were reported for a decrease in XyG fucosylation neither in *mur2* mutants (Vanzin et al., 2002) nor in plants overexpressing *AXY8* (Günl et al., 2011). However, in the absence of functional ABP1, the partial restoration of elongation resulting from *AXY8* overexpression in these plants revealed that defucosylation of XyG is required for hypocotyl elongation in darkness (Figure 6). These data highlight the importance of tight regulation of XyG side chain fucosylation for expansion. This effect can be observed after ABP1 inactivation thanks to the specific signature of gene expression in this background, especially for genes involved either in the metabolism of XyG or in XyG-cellulose interactions. Reciprocally, the combination of altered gene expression after ABP1 inactivation might have significantly reduced possibilities for compensation; thus, in this background, changes in critical cell wall components generate obvious developmental defects (Supplemental Figure 9).

ABP1 and Oligosaccharins

Group III-A *XTH* genes, which include *XTH31* and *XTH32*, were induced after inactivation of ABP1, whereas many other *XTH*s, except *XTH7*, were repressed. *XTH31* and *XTH32* encode proteins exhibiting predominantly xyloglucan hydrolase activity (Maris et al., 2011). ABP1 inactivated hypocotyl might have an increased XEH activity, thus increasing XyG hydrolysis. Cleavage of hyperfucosylated XyG would release an increased amount of fucosylated oligosaccharides, which can act as signaling molecules and affect cell elongation (Fry et al., 1993; Fry, 1994). Within such oligosaccharides, the Fuc residue is not strictly required to promote growth but XXFG fragments were the most effective to stimulate growth in pea (*Pisum sativum*) stems (McDougall and Fry, 1989). Interestingly, XXFG was shown to antagonize the promotive effect of the synthetic auxin 2,4-D on growth of pea stem segments, whereas fragments lacking Fuc were not able to counterbalance the auxin effect (York et al., 1984; McDougall and Fry, 1989; Augur et al., 1993). Based on these observations, it is tempting to hypothesize that, in plants inactivated for ABP1, the inhibition of hypocotyl lengthening partially results from an increase in fucosylated oligosaccharides. That might be an explanation for the partial restoration of hypocotyl elongation after overexpression of the α-fucosidase AXY8; however, it is much less likely when considering the lack of growth restoration by *mur2* mutation, except if there is a tight specificity of XEHs for XyG substrates. There is currently no evidence supporting the idea that XEHs differentially hydrolyze fucosylated versus nonfucosylated XyG. We cannot rule out that ABP1 somehow affects the relative amount of oligosaccharins produced at the cell wall by controlling the expression of XTHs but determining whether it can account for the observed difference between AXY8 overexpression and *mur2* mutation is still unclear.

ABP1 Differentiates between XyG Biosynthesis and Metabolism

As indicated above, a critical difference was observed after ABP1 inactivation between the defect in fucosylated XyG biosynthesis in the *mur2* mutant and removal of XyG Fuc within the cell wall by the apoplastic α-fucosidase AXY8 (Figure 6). In the first case, no restoration of hypocotyl growth was observed, whereas in muro defucosylation efficiently restored cell elongation. Beyond the information on the importance of XyG fucosylation modification, this observation reveals that acting primarily on XyG biosynthesis diverges significantly from affecting XyG metabolism within the cell wall. Various and nonexclusive scenarios might explain the basis for such a difference. First, the substitution pattern of newly synthetized XyGs, typically the presence or absence of Fuc on the side chains, might affect their incorporation into the polymer. Second, the length and nature of side chains are predicted to modify the XyG-cellulose microfibril network. Analysis and modeling of XyG-cellulose interaction indicated that all XyGs were able to interact with cellulose, but the length and nature of the side chains modify their interface and resultant conformations

(Pauly et al., 1999; Bootten et al., 2004; Hanus and Mazeau, 2006; Whitney et al., 2006; Dick-Perez et al., 2011; Park and Cosgrove, 2012b). The nature and diversity of XyG substitutions are potentially responsible for the reported or predicted behaviors of XyG (Pauly et al., 1999). Integrating nonfucosylated (as in *mur2-1*) or fucosylated XyG into XyG polymers might then change the XyG-cellulose microfibril network. Third, XyG fucosylation and acetylation, and resulting changes in XyG and XyG-cellulose network conformations, might also affect the accessibility or substrate specificity to cell wall A-type expansins or XTH enzymes. To date, little is known about the possible specificity of various XTHs toward XyG motifs. Many members of these two gene families were found to be differentially expressed after inactivation of ABP1, and we can hypothesize that these changes affect XyG remodeling. During hypocotyl growth in darkness, the elongation zone of the hypocotyl progresses from the base to the upper part of the hypocotyl and cells undergo progressive changes in cell wall characteristics accordingly. Interestingly, ABP1-dependent regulation of the fucosylation/defucosylation combined with modification of gene expression might be an efficient mechanism to control and coordinate cell elongation in time and space.

METHODS

Plant Lines and Growth Conditions

Wild-type Columbia-0 (Col-0) ecotype of *Arabidopsis thaliana* and conditional lines for ABP1 (SS12K and SS12S that express the recombinant antibody scFv12 blocking ABP1 function or the antisense line AS9) were surface sterilized and grown under sterile conditions on plates containing half-strength Murashige and Skoog basal salt mixture, buffered at pH 5.7 with 2.5 mM MES, and containing 0.9% vitro agar (Kalys). After stratification, plates were exposed 4 h to light and transferred to a vertical position at 22°C for 4 d in darkness. These growth conditions were obtained using a dedicated growth chamber placed in a dark room equipped with green light. The wild type and SS12K were grown in the same plate for growth and cell wall composition analyses. Ethanol induction was performed at the indicated time by exposure of siblings to ethanol vapors coming from a microtube containing 500 μL of 5% ethanol, placed at the bottom of each square plate. Plates were sealed with Parafilm to hold the vapors in the plate (Supplemental Figure 1C). Inductions were performed either immediately after stratification of the seeds, 24 or 8 h before harvesting the seedlings.

SS12K was crossed with *mur2-1* (Vanzin et al., 2002) and *tir1-1 afb2-1 afb3-1* (Dharmasiri et al., 2005) mutants or with *p35S:AXY8* overexpressor (Günl et al., 2011), *p35S:PIP2;1-GFP* (for green fluorescent protein; Luu et al., 2012), and *pCESA6:UidA* (Desprez et al., 2007) to introgress the ethanol inducible scFv12 construct into the corresponding background. Double homozygotes were selected for growth and cell wall analyses except for 35S:AXY8 SS12K where heterozygous plants were used.

Cell Measurements and GUS Staining

Epidermal cell length of Col-0 and SS12K hypocotyls were performed using plants exhibiting *p35S:PIP2,1-GFP* construct (Luu et al., 2012). Dark-grown seedlings of 2, 3, and 4 d were observed using an inverted confocal microscope TCS SP2 (Leica Microsystems). Hypocotyls were reconstructed using Photoshop, and cell lengths were measured using ImageJ software (NIH).

The GUS assays were performed as previously described (Tromas et al., 2009). Two- and four-day-old dark-grown seedlings of Col-0 and SS12K harboring the *pCESA6:UidA* construct were stained during 3 h at 37°C. GUS-stained seedlings were observed without clearing with a MultiZoom AZ100 microscope (Nikon Instruments) under bright field.

Hypocotyl length measurements were made on high-resolution scans of each plate using ImageJ software, at exactly 4 d of growth. Mean length was obtained from four biological repeats in duplicates grown in parallel to material for cell wall analysis.

Transmission Electron Microscopy and Measurement of Cell Wall Thickness

Three-day-old dark-grown seedlings of Col-0 and SS12K were collected and fixed overnight at room temperature in 3% (w/v) glutaraldehyde/1% (w/v) paraformaldehyde in 0.2 M sodium cacodylate, pH 6.8, under gentle agitation. After three washes in the same buffer at 0.1 M, seedlings were postfixed in 1% (w/v) osmium tetroxide/1.5% potassium ferrocyanide (w/v) in water for 1 h. After extensive washes in water, seedlings were dissected under water to select hypocotyl fragments from the base and the elongation zone. Fragments were dehydrated through graded ethanol series and then embedded in epoxy resin (agar low-viscosity premix kit medium; Oxford Instruments) and polymerized for 20 h at 60°C.

Transversal ultrathin sections (~90 nm) of embedded material were cut using an ultramicrotome (Ultracut UC6; Leica) and were picked up onto 200 mesh, Formvar-coated copper grids. Sections were stained with aqueous 2% (w/v) uranyl acetate for 20 min, rinsed, and then silver stained for 6 min. Grids were examined under a JEOL 1400 TEM operating at 120 kV. Images were acquired using a postcolumn high-resolution (11 megapixels) high-speed camera (SC1000 Orius; Gatan).

Cell wall thickness was measured on images previously acquired from three hypocotyls of each genotype using ImageJ software.

Hypocotyl transverse semithin sections of SS12K (~300 nm) were stained by toluidine blue and observed with a BX53 microscope (Olympus). Images were captured with an Olympus DP73 digital camera.

Microarray Analysis

Four-day-old dark-grown seedlings of Col-0 and SS12K ABP1 conditional line were harvested under green light at day 4 (96 h) after culture in the dark. Seedlings were induced by ethanol vapor either since their transfer to darkness or 8 h before harvesting. RNA was extracted using a Qiagen RNeasy kit and digested with RNase free DNase on the column following the manufacturer's instructions, and RNA quantification and quality control were achieved using 2100 Bioanalyzer RNA chip (Agilent). Three independent biological replicates were used for each condition.

RNA labeling, hybridization of 70-mer oligonucleotide arrays with the Qiagen-Operon *Arabidopsis* Genome Array Ready Oligo Set (AROS) version 3.0 (http://www.ag.arizona.edu/microarray/), and data analysis were as previously described (Stavang et al., 2009). Microarray slides were scanned with a GenePix 4000B scanner (Axon Molecular Devices). Spot intensities were quantified using Genepix Pro 6.0 software (Axon Molecular Devices), and those with a net intensity in both channels lower than the median signal background plus twice the standard deviations were removed as low-signal spots. Data were normalized by median global intensity and with LOWESS correction (Yang et al., 2002) with Genepix Pro 6.0 and Acuity 4.0 software (Axon Molecular Devices), respectively. Microarray raw data have been deposited in the National Center for Biotechnology Information's Gene Expression Omnibus database under accession number GSE46196.

Monosaccharide Composition and Linkage Analysis of Polysaccharides

The analyses of polysaccharides were performed on an alcohol-insoluble material prepared as follows. Two grams (fresh weight) of 4-d-old dark-

grown hypocotyl were washed twice in 4 volumes of absolute ethanol for 15 min, then rinsed twice in 4 volumes of acetone at room temperature for 10 min and left to dry under a fume hood overnight at room temperature.

Neutral monosaccharide composition and uronic acid quantification were performed on 10 mg of dried alcohol-insoluble material after hydrolysis in 2.5 M trifluoroacetic acid for 1 h at 100°C as described by Harholt et al. (2006) and Blumenkrantz and Asboe-Hansen (1973), respectively. The linkage analysis was performed on 500 µg of alcohol-insoluble material as described (Eudes et al., 2008). To determine the cellulose content, the residual pellet obtained after the monosaccharide analysis was rinsed twice with 10 volumes of water and hydrolyzed with H_2SO_4 as described (Updegraff, 1969). The released Glc was diluted 500 times and then quantified using an HPAEC-PAD chromatography as described (Harholt et al., 2006).

Xyloglucan Fingerprinting (OLIMP)

Dark-grown seedlings were collected under green light and stored in cold ethanol. For each biological repeat, five hypocotyls were dissected and used for the analysis. After one night at room temperature in ethanol, the ethanol was removed and hypocotyls were dried at 37°C for 1 h. Twenty microliters of 50 mM acetate buffer, pH 5.0, containing endoglucanase from *Trichoderma longibrachiatum* (Magzyme) was then added and left overnight at 37°C. OLIMP was then performed as reported (Lerouxel et al., 2002) using Super DHB matrix (9:1 mixture of DHB and 2-hydroxy-5-methoxybenzoic acid; Fluka) instead of DHB.

Starch Staining

Four-day-old dark-grown seedlings of Col-0, SS12K, and *cop10-4* were incubated in Lugol's iodine solution (6 mM iodine, 43 mM KI, and 0.2 N HCl) to detect starch granules.

Real-Time RT-PCR Analysis

RNA was extracted from 4-d-old dark-grown seedlings using an Qiagen RNeasy kit and digested with RNase-free DNase on the column following the manufacturer's instructions (Qiagen). First-strand cDNAs were synthesized from 5 µg of total RNA using SuperScript III reverse transcriptase according to the manufacturer's instructions (Invitrogen). Quantitative RT-PCR analyses were performed using LightCycler 480 SYBR Green I master mix (Roche) with specific primers as presented Supplemental Table 1. PCR cycling conditions for amplification were 95°C for 10 min, then 40 to 50 cycles of 95°C for 15 s, 62°C for 15 s, and 72°C for 15 s followed by $0.1°C \cdot s^{-1}$ ramping up to 95°C for fusion curve characterization. Three biological repeats were analyzed in duplicates. Each sample was normalized with *ACTIN2-8*, and data are expressed in relative units to *ACTIN*.

Statistics

Classical statistical analyses were performed using either Student's *t* test or nonparametric Kruskal-Wallis analysis according to experimental constraints.

Accession Numbers

Sequence data from this article can be found in the Arabidopsis Genome Initiative or GenBank/EMBL databases under the following accession numbers: At1g70230, At4g34260, At3g13750, At3g52840, At5g63800, At2g28470, At5g64570, At1g69530, At1g26770, At5g56320, At4g38210, At2g39700, At3g29030, At3g45970, At1g67830, At2g03220, At2g20370, At4g37800, At1g11545, At4g30290, At4g25810, At1g32170, At3g44990, At2g36870, At1g10550, At4g37800, and At1g11545, At1g68560.

Supplemental Data

The following materials are available in the online version of this article.

Supplemental Figure 1. Dark-Grown Phenotype of Various ABP1 Knockdown Lines.

Supplemental Figure 2. Overview of Classes of Genes Differentially Expressed after ABP1 Inactivation in Dark-Grown Seedlings Ordered by Cellular Component.

Supplemental Figure 3. Expression of Cell Wall–Related Genes after Ethanol Induction in the Wild Type.

Supplemental Figure 4. Venn Diagram Resulting from Meta-Analysis Comparing Genes Affected in ABP1 Knockdown with Genes Affected in Deetiolated Seedlings Resulting from Alteration in GA, BR, or Light Signaling.

Supplemental Figure 5. Comparison of Xyloglucan Composition of Dark-Grown Hypocotyls of the *cop10-4* Deetiolated Mutant with the Wild Type.

Supplemental Figure 6. Xyloglucan Composition in Dark-Grown Hypocotyls of Various Lines Inactivated for ABP1.

Supplemental Figure 7. XyG Gene Expression Analyzed by Real-Time RT-PCR.

Supplemental Figure 8. Auxin Effect on Expression of XyG Remodeling Genes.

Supplemental Figure 9. ABP1 Acts upon in Muro Xyloglucan Composition to Modulate Cell Expansion through an $SCF^{TIR/AFB}$-Dependent Pathway.

Supplemental Table 1. List of Primers Used in Real-Time RT-PCR.

Supplemental Data Set 1. List of Cell Wall Genes Differentially Expressed between the Wild Type and SS12K.

Supplemental Data Set 2. List of Cell Wall Genes Shared with Other Deetiolated Seedlings.

ACKNOWLEDGMENTS

We thank Markus Pauly (University of California, Berkeley) for kindly providing the seeds of AXY8 overexpressor, Mark Estelle (University of California, San Diego, Howard Hughes Medical Institute) for seeds of the triple *tir afb2 afb3* mutant, Xing Wang Deng (Yale University) for seeds of *cop10-4*, Doan Luu (CNRS, Montpellier) for seeds of the 35S:PIP2;1-GFP line, and Jiří Friml (Institute of Science and Technology, Vienna) for seeds of the *abp1-5* mutant. We thank Sylvie Citerne from the Plant Observatory at Institut Jean-Pierre Bourgin (INRA) for cell wall composition analysis. This work has benefitted from the facilities and expertise of the Imagif Cell Biology Unit of the Gif campus, which is supported by the Conseil Général de l'Essonne, France. We also thank Jessica Marion for technical assistance in electron microscopy. This work was supported by the ANR blanc AuxiWall Project ANR-11-BSV5-0007. C.P.-R.'s team is also funded by the CNRS and G.M. by INRA. Work in the laboratories of D.A. and M.A.B. was supported by grants from the Spanish Ministry of Science and Innovation (BIO2010-15071 and CSD2007-00057) and the Generalitat Valenciana (ACOMP/2011/288 and PROMETEO/2010/020). We thank Philip Harris (University of Auckland) and Spencer Brown (Institut des Sciences du Végétal, CNRS) for critical reading of the article and useful comments.

AUTHOR CONTRIBUTIONS

S.P., G.M., and C.P.-R. designed the research. S.P., L.G., C.G., D.A., C.P.-B., P.M., A.G., and R.S. performed research. S.P., D.A., and M.A.B.

performed transcriptomic analysis. S.P., L.G., G.M., and C.P.-R. analyzed data. S.P. and C.P.-R. wrote the article with critical reading from G.M., D.A., and M.B.

Received October 24, 2013; revised October 24, 2013; accepted December 19, 2013; published January 14, 2014.

REFERENCES

Anderson, C.T., Carroll, A., Akhmetova, L., and Somerville, C. (2010). Real-time imaging of cellulose reorientation during cell wall expansion in Arabidopsis roots. Plant Physiol. **152:** 787–796.

Augur, C., Benhamou, N., Darvill, A., and Albersheim, P. (1993). Purification, characterization, and cell wall localization of an alpha-fucosidase that inactivates a xyloglucan oligosaccharin. Plant J. **3:** 415–426.

Barbier-Brygoo, H., Zimmermann, S., Thomine, S., White, I.R., Millner, P., and Guern, J. (1996). Elementary auxin response chains at the plasma membrane involve external abp1 and multiple electrogenic ion transport proteins. Plant Growth Regul. **18:** 23–28.

Baumann, M.J., Eklöf, J.M., Michel, G., Kallas, A.M., Teeri, T.T., Czjzek, M., and Brumer, H.I., III., (2007). Structural evidence for the evolution of xyloglucanase activity from xyloglucan endo-transglycosylases: Biological implications for cell wall metabolism. Plant Cell **19:** 1947–1963.

Blumenkrantz, N., and Asboe-Hansen, G. (1973). New method for quantitative determination of uronic acids. Anal. Biochem. **54:** 484–489.

Bootten, T.J., Harris, P.J., Melton, L.D., and Newman, R.H. (2004). Solid-state 13C-NMR spectroscopy shows that the xyloglucans in the primary cell walls of mung bean (*Vigna radiata* L.) occur in different domains: A new model for xyloglucan-cellulose interactions in the cell wall. J. Exp. Bot. **55:** 571–583.

Braun, N., Wyrzykowska, J., Muller, P., David, K., Couch, D., Perrot-Rechenmann, C., and Fleming, A.J. (2008). Conditional repression of AUXIN BINDING PROTEIN1 reveals that it coordinates cell division and cell expansion during postembryonic shoot development in *Arabidopsis* and tobacco. Plant Cell **20:** 2746–2762.

Calderón Villalobos, L.I., et al. (2012). A combinatorial TIR1/AFB-Aux/IAA co-receptor system for differential sensing of auxin. Nat. Chem. Biol. **8:** 477–485.

Cavalier, D.M., Lerouxel, O., Neumetzler, L., Yamauchi, K., Reinecke, A., Freshour, G., Zabotina, O.A., Hahn, M.G., Burgert, I., Pauly, M., Raikhel, N.V., and Keegstra, K. (2008). Disrupting two *Arabidopsis thaliana* xylosyltransferase genes results in plants deficient in xyloglucan, a major primary cell wall component. Plant Cell **20:** 1519–1537.

Chapman, E.J., and Estelle, M. (2009). Mechanism of auxin-regulated gene expression in plants. Annu. Rev. Genet. **43:** 265–285.

Chen, J.G., Ullah, H., Young, J.C., Sussman, M.R., and Jones, A.M. (2001). ABP1 is required for organized cell elongation and division in Arabidopsis embryogenesis. Genes Dev. **15:** 902–911.

Christian, M., Steffens, B., Schenck, D., Burmester, S., Böttger, M., and Lüthen, H. (2006). How does auxin enhance cell elongation? Roles of auxin-binding proteins and potassium channels in growth control. Plant Biol. (Stuttg.) **8:** 346–352.

Cosgrove, D.J. (2000). Loosening of plant cell walls by expansins. Nature **407:** 321–326.

Cosgrove, D.J. (2005). Growth of the plant cell wall. Nat. Rev. Mol. Cell Biol. **6:** 850–861.

David, K.M., Couch, D., Braun, N., Brown, S., Grosclaude, J., and Perrot-Rechenmann, C. (2007). The auxin-binding protein 1 is essential for the control of cell cycle. Plant J. **50:** 197–206.

Desprez, T., Juraniec, M., Crowell, E.F., Jouy, H., Pochylova, Z., Parcy, F., Höfte, H., Gonneau, M., and Vernhettes, S. (2007). Organization of cellulose synthase complexes involved in primary cell wall synthesis in *Arabidopsis thaliana*. Proc. Natl. Acad. Sci. USA **104:** 15572–15577.

Dharmasiri, N., Dharmasiri, S., Weijers, D., Lechner, E., Yamada, M., Hobbie, L., Ehrismann, J.S., Jürgens, G., and Estelle, M. (2005). Plant development is regulated by a family of auxin receptor F box proteins. Dev. Cell **9:** 109–119.

Dick-Perez, M., Zhang, Y., Hayes, J., Salazar, A., Zabotina, O.A., and Hong, M. (2011). Structure and interactions of plant cell-wall polysaccharides by two- and three-dimensional magic-angle-spinning solid-state NMR. Biochemistry **50:** 989–1000.

Effendi, Y., Rietz, S., Fischer, U., and Scherer, G.F. (2011). The heterozygous abp1/ABP1 insertional mutant has defects in functions requiring polar auxin transport and in regulation of early auxin-regulated genes. Plant J. **65:** 282–294.

Esmon, C.A., Tinsley, A.G., Ljung, K., Sandberg, G., Hearne, L.B., and Liscum, E. (2006). A gradient of auxin and auxin-dependent transcription precedes tropic growth responses. Proc. Natl. Acad. Sci. USA **103:** 236–241.

Eudes, A., Mouille, G., Thévenin, J., Goyallon, A., Minic, Z., and Jouanin, L. (2008). Purification, cloning and functional characterization of an endogenous beta-glucuronidase in *Arabidopsis thaliana*. Plant Cell Physiol. **49:** 1331–1341.

Franková, L., and Fry, S.C. (2011). Phylogenetic variation in glycosidases and glycanases acting on plant cell wall polysaccharides, and the detection of transglycosidase and trans-β-xylanase activities. Plant J. **67:** 662–681.

Fry, S.C. (1994). Oligosaccharins as plant growth regulators. Biochem. Soc. Symp. **60:** 5–14.

Fry, S.C., Aldington, S., Hetherington, P.R., and Aitken, J. (1993). Oligosaccharides as signals and substrates in the plant cell wall. Plant Physiol. **103:** 1–5.

Fry, S.C., McDougall, G.J., Lorences, E.P., Biggs, K.J., and Smith, R.C. (1990). Oligosaccharins from xyloglucan and cellulose: Modulators of the action of auxin and H+ on plant growth. Symp. Soc. Exp. Biol. **44:** 285–298.

Gallego-Bartolomé, J., Minguet, E.G., Grau-Enguix, F., Abbas, M., Locascio, A., Thomas, S.G., Alabadí, D., and Blázquez, M.A. (2012). Molecular mechanism for the interaction between gibberellin and brassinosteroid signaling pathways in Arabidopsis. Proc. Natl. Acad. Sci. USA **109:** 13446–13451.

Gendreau, E., Traas, J., Desnos, T., Grandjean, O., Caboche, M., and Höfte, H. (1997). Cellular basis of hypocotyl growth in *Arabidopsis thaliana*. Plant Physiol. **114:** 295–305.

Günl, M., Neumetzler, L., Kraemer, F., de Souza, A., Schultink, A., Pena, M., York, W.S., and Pauly, M. (2011). AXY8 encodes an α-fucosidase, underscoring the importance of apoplastic metabolism on the fine structure of *Arabidopsis* cell wall polysaccharides. Plant Cell **23:** 4025–4040.

Hanus, J., and Mazeau, K. (2006). The xyloglucan-cellulose assembly at the atomic scale. Biopolymers **82:** 59–73.

Harholt, J., Jensen, J.K., Sørensen, S.O., Orfila, C., Pauly, M., and Scheller, H.V. (2006). ARABINAN DEFICIENT 1 is a putative arabinosyltransferase involved in biosynthesis of pectic arabinan in Arabidopsis. Plant Physiol. **140:** 49–58.

Hsieh, Y.S., and Harris, P.J. (2012). Structures of xyloglucans in primary cell walls of gymnosperms, monilophytes (ferns sensu lato) and lycophytes. Phytochemistry **79:** 87–101.

Iglesias, N., Abelenda, J.A., Rodiño, M., Sampedro, J., Revilla, G., and Zarra, I. (2006). Apoplastic glycosidases active against xyloglucan oligosaccharides of *Arabidopsis thaliana*. Plant Cell Physiol. **47:** 55–63.

Jamet, E., Roujol, D., San-Clemente, H., Irshad, M., Soubigou-Taconnat, L., Renou, J.P., and Pont-Lezica, R. (2009). Cell wall biogenesis of *Arabidopsis thaliana* elongating cells: Transcriptomics complements proteomics. BMC Genomics **10:** 505.

Jones, A.M., Im, K.H., Savka, M.A., Wu, M.J., DeWitt, N.G., Shillito, R., and Binns, A.N. (1998). Auxin-dependent cell expansion mediated by overexpressed auxin-binding protein 1. Science **282:** 1114–1117.

Leblanc, N., David, K., Grosclaude, J., Pradier, J.M., Barbier-Brygoo, H., Labiau, S., and Perrot-Rechenmann, C. (1999b). A novel immunological approach establishes that the auxin-binding protein, Nt-abp1, is an element involved in auxin signaling at the plasma membrane. J. Biol. Chem. **274:** 28314–28320.

Leblanc, N., Perrot-Rechenmann, C., and Barbier-Brygoo, H. (1999a). The auxin-binding protein Nt-ERabp1 alone activates an auxin-like transduction pathway. FEBS Lett. **449:** 57–60.

Lerouxel, O., Cavalier, D.M., Liepman, A.H., and Keegstra, K. (2006). Biosynthesis of plant cell wall polysaccharides - A complex process. Curr. Opin. Plant Biol. **9:** 621–630.

Lerouxel, O., Choo, T.S., Séveno, M., Usadel, B., Faye, L., Lerouge, P., and Pauly, M. (2002). Rapid structural phenotyping of plant cell wall mutants by enzymatic oligosaccharide fingerprinting. Plant Physiol. **130:** 1754–1763.

Levy, S., Maclachlan, G., and Staehelin, L.A. (1997). Xyloglucan sidechains modulate binding to cellulose during in vitro binding assays as predicted by conformational dynamics simulations. Plant J. **11:** 373–386.

Lewis, D.R., Olex, A.L., Lundy, S.R., Turkett, W.H., Fetrow, J.S., and Muday, G.K. (2013). A kinetic analysis of the auxin transcriptome reveals cell wall remodeling proteins that modulate lateral root development in *Arabidopsis*. Plant Cell **25:** 3329–3346.

Lorenzo, O., Piqueras, R., Sánchez-Serrano, J.J., and Solano, R. (2003). ETHYLENE RESPONSE FACTOR1 integrates signals from ethylene and jasmonate pathways in plant defense. Plant Cell **15:** 165–178.

Luu, D.T., Martinière, A., Sorieul, M., Runions, J., and Maurel, C. (2012). Fluorescence recovery after photobleaching reveals high cycling dynamics of plasma membrane aquaporins in Arabidopsis roots under salt stress. Plant J. **69:** 894–905.

Ma, L., Gao, Y., Qu, L., Chen, Z., Li, J., Zhao, H., and Deng, X.W. (2002). Genomic evidence for COP1 as a repressor of light-regulated gene expression and development in *Arabidopsis*. Plant Cell **14:** 2383–2398.

Maris, A., Kaewthai, N., Eklöf, J.M., Miller, J.G., Brumer, H., Fry, S.C., Verbelen, J.P., and Vissenberg, K. (2011). Differences in enzymic properties of five recombinant xyloglucan endotransglucosylase/hydrolase (XTH) proteins of *Arabidopsis thaliana*. J. Exp. Bot. **62:** 261–271.

McDougall, G.J., and Fry, S.C. (1989). Structure-activity relationships for xyloglucan oligosaccharides with antiauxin activity. Plant Physiol. **89:** 883–887.

Nemhauser, J.L., Hong, F., and Chory, J. (2006). Different plant hormones regulate similar processes through largely nonoverlapping transcriptional responses. Cell **126:** 467–475.

Okushima, Y., et al. (2005). Functional genomic analysis of the AUXIN RESPONSE FACTOR gene family members in *Arabidopsis thaliana*: Unique and overlapping functions of ARF7 and ARF19. Plant Cell **17:** 444–463.

Overvoorde, P.J., et al. (2005). Functional genomic analysis of the AUXIN/INDOLE-3-ACETIC ACID gene family members in *Arabidopsis thaliana*. Plant Cell **17:** 3282–3300.

Pauly, M., Albersheim, P., Darvill, A., and York, W.S. (1999). Molecular domains of the cellulose/xyloglucan network in the cell walls of higher plants. Plant J. **20:** 629–639.

Park, Y.B., and Cosgrove, D.J. (2012a). Changes in cell wall biomechanical properties in the xyloglucan-deficient xxt1/xxt2 mutant of Arabidopsis. Plant Physiol. **158:** 465–475.

Park, Y.B., and Cosgrove, D.J. (2012b). A revised architecture of primary cell walls based on biomechanical changes induced by substrate-specific endoglucanases. Plant Physiol. **158:** 1933–1943.

Pauly, M., Qin, Q., Greene, H., Albersheim, P., Darvill, A., and York, W.S. (2001). Changes in the structure of xyloglucan during cell elongation. Planta **212:** 842–850.

Peña, M.J., Ryden, P., Madson, M., Smith, A.C., and Carpita, N.C. (2004). The galactose residues of xyloglucan are essential to maintain mechanical strength of the primary cell walls in Arabidopsis during growth. Plant Physiol. **134:** 443–451.

Pufky, J., Qiu, Y., Rao, M.V., Hurban, P., and Jones, A.M. (2003). The auxin-induced transcriptome for etiolated Arabidopsis seedlings using a structure/function approach. Funct. Integr. Genomics **3:** 135–143.

Rayle, D.L., and Cleland, R.E. (1992). The Acid Growth Theory of auxin-induced cell elongation is alive and well. Plant Physiol. **99:** 1271–1274.

Robert, S., et al. (2010). ABP1 mediates auxin inhibition of clathrin-dependent endocytosis in Arabidopsis. Cell **143:** 111–121.

Rose, J.K., Braam, J., Fry, S.C., and Nishitani, K. (2002). The XTH family of enzymes involved in xyloglucan endotransglucosylation and endohydrolysis: current perspectives and a new unifying nomenclature. Plant Cell Physiol. **43:** 1421–1435.

Ryden, P., Sugimoto-Shirasu, K., Smith, A.C., Findlay, K., Reiter, W.D., and McCann, M.C. (2003). Tensile properties of Arabidopsis cell walls depend on both a xyloglucan cross-linked microfibrillar network and rhamnogalacturonan II-borate complexes. Plant Physiol. **132:** 1033–1040.

Salisbury, F.B., Gillespie, L., and Rorabaugh, P. (1988). Gravitropism in higher plant shoots. V. Changing sensitivity to auxin. Plant Physiol. **88:** 1186–1194.

Stavang, J.A., Gallego-Bartolomé, J., Gómez, M.D., Yoshida, S., Asami, T., Olsen, J.E., García-Martínez, J.L., Alabadí, D., and Blázquez, M.A. (2009). Hormonal regulation of temperature-induced growth in Arabidopsis. Plant J. **60:** 589–601.

Steffens, B., Feckler, C., Palme, K., Christian, M., Böttger, M., and Lüthen, H. (2001). The auxin signal for protoplast swelling is perceived by extracellular ABP1. Plant J. **27:** 591–599.

Stepanova, A.N., Yun, J., Likhacheva, A.V., and Alonso, J.M. (2007). Multilevel interactions between ethylene and auxin in *Arabidopsis* roots. Plant Cell **19:** 2169–2185.

Swarup, K., et al. (2008). The auxin influx carrier LAX3 promotes lateral root emergence. Nat. Cell Biol. **10:** 946–954.

Takeda, T., Furuta, Y., Awano, T., Mizuno, K., Mitsuishi, Y., and Hayashi, T. (2002). Suppression and acceleration of cell elongation by integration of xyloglucans in pea stem segments. Proc. Natl. Acad. Sci. USA **99:** 9055–9060.

Tamura, K., Shimada, T., Kondo, M., Nishimura, M., and Hara-Nishimura, I. (2005). KATAMARI1/MURUS3 is a novel Golgi membrane protein that is required for endomembrane organization in *Arabidopsis*. Plant Cell **17:** 1764–1776.

Thiel, G., Blatt, M.R., Fricker, M.D., White, I.R., and Millner, P. (1993). Modulation of K+ channels in Vicia stomatal guard cells by peptide homologs to the auxin-binding protein C terminus. Proc. Natl. Acad. Sci. USA **90:** 11493–11497.

Tromas, A., Braun, N., Muller, P., Khodus, T., Paponov, I.A., Palme, K., Ljung, K., Lee, J.Y., Benfey, P., Murray, J.A., Scheres, B., and Perrot-Rechenmann, C. (2009). The AUXIN BINDING PROTEIN 1 is required for differential auxin responses mediating root growth. PLoS ONE **4:** e6648.

Tromas, A., Paque, S., Stierlé, V., Quettier, A.L., Muller, P., Lechner, E., Genschik, P., and Perrot-Rechenmann, C. (2013). Auxin-binding protein 1 is a negative regulator of the SCF(TIR1/AFB) pathway. Nat Commun **4:** 2496–2504.

Updegraff, D.M. (1969). Semimicro determination of cellulose in biological materials. Anal. Biochem. **32:** 420–424.

Vanzin, G.F., Madson, M., Carpita, N.C., Raikhel, N.V., Keegstra, K., and Reiter, W.D. (2002). The mur2 mutant of Arabidopsis thaliana lacks fucosylated xyloglucan because of a lesion in fucosyltransferase AtFUT1. Proc. Natl. Acad. Sci. USA **99:** 3340–3345.

Vissenberg, K., Oyama, M., Osato, Y., Yokoyama, R., Verbelen, J. P., and Nishitani, K. (2005). Differential expression of AtXTH17, AtXTH18, AtXTH19 and AtXTH20 genes in Arabidopsis roots. Physiological roles in specification in cell wall construction. Plant Cell Physiol. **46:** 192–200.

Whitney, S.E., Wilson, E., Webster, J., Bacic, A., Reid, J.S., and Gidley, M.J. (2006). Effects of structural variation in xyloglucan polymers on interactions with bacterial cellulose. Am. J. Bot. **93:** 1402–1414.

Wolf, S., Hématy, K., and Höfte, H. (2012). Growth control and cell wall signaling in plants. Annu. Rev. Plant Biol. **63:** 381–407.

Xu, T., Wen, M., Nagawa, S., Fu, Y., Chen, J.G., Wu, M.J., Perrot-Rechenmann, C., Friml, J., Jones, A.M., and Yang, Z. (2010). Cell surface- and rho GTPase-based auxin signaling controls cellular interdigitation in Arabidopsis. Cell **143:** 99–110.

Yang, Y.H., Dudoit, S., Luu, P., Lin, D.M., Peng, V., Ngai, J., and Speed, T.P. (2002). Normalization for cDNA microarray data: a robust composite method addressing single and multiple slide systematic variation. Nucleic Acids Res. **30:** e15.

York, W.S., Darvill, A.G., and Albersheim, P. (1984). Inhibition of 2,4-dichlorophenoxyacetic acid-stimulated elongation of pea stem segments by a xyloglucan oligosaccharide. Plant Physiol. **75:** 295–297.

Zablackis, E., York, W.S., Pauly, M., Hantus, S., Reiter, W.D., Chapple, C.C., Albersheim, P., and Darvill, A. (1996). Substitution of L-fucose by L-galactose in cell walls of Arabidopsis mur1. Science **272:** 1808–1810.

Zabotina, O.A. (2012). Xyloglucan and its biosynthesis. Front. Plant Sci. **3:** 134.

Zabotina, O.A., van de Ven, W.T., Freshour, G., Drakakaki, G., Cavalier, D., Mouille, G., Hahn, M.G., Keegstra, K., and Raikhel, N.V. (2008). Arabidopsis XXT5 gene encodes a putative alpha-1,6-xylosyltransferase that is involved in xyloglucan biosynthesis. Plant J. **56:** 101–115.